

Electronic Supplementary Information

Designing Efficient $\text{Bi}_2\text{Fe}_4\text{O}_9$ Photoanodes via Bulk and Surface Defect Engineering

*Sabiha Akter Monny, Zhiliang Wang, * Tongen Lin, Peng Chen, Bin Luo, Lianzhou Wang**

^a Nanomaterials Centre, School of Chemical Engineering and

Australian Institute for Bioengineering and Nanotechnology

The University of Queensland

St Lucia, QLD 4072, Australia

*E-mail: zhiliang.wang@uq.edu.au; l.wang@uq.edu.au

Experimental section

Photoelectrode fabrication

N₂ treated and pure Bi₂Fe₄O₉. Bi₂Fe₄O₉ thin films were fabricated on fluorine doped tin oxide (FTO) substrate by spin coating method. The precursor solution was prepared by dissolving 0.2 M Bi(NO₃)₃·5H₂O, 0.4 M Fe(NO₃)₃·9H₂O, 1.9 M citric acid in 2-methoxyethanol. The solution was stirred continuously for 1 hour at 70 °C. The films were then prepared by spin coating the precursor solution on FTO substrate at 3000 rpm for 30 s and then heated on hotplate at 400 °C for 7 minutes. These steps were repeated 9 times to increase the film thickness. Then the as prepared electrodes were calcined in a tube furnace at 600 °C (ramping rate 2 °C min⁻¹) for 2 h in N₂ atmosphere, sample noted as BFO-N. Alternatively, the samples are calcined in air at 600 °C (2 °C min⁻¹) for 2 hours, noted as BFO.

HCl acid treatment. The as-prepared BFO-N electrode was immersed in 5 M HCl aqueous solution (32 %) for varying time (e.g 10 s, 20 s, 30 s), then washed with DI water and dried in N₂ stream, noted as HCl-BFO-N. The best acid treatment time is 20 s.

CoPi deposition. Photo-assisted electrodeposition of cobalt phosphate (CoPi) on Bi₂Fe₄O₉ electrode was carried out by a previously reported method.¹ A constant current density of 0.75 μA cm⁻² was applied in a solution of 0.5 mM Co(NO₃)₂·6H₂O in 0.1 M potassium phosphate buffer at pH 7 under AM 1.5G irradiation (100 mW cm⁻²). The amount of CoPi was controlled by the deposition time, which ranged between 150 and 250 s. The photoanode was then rinsed with distilled water, noted as CoPi/HCl-BFO-N. The best deposition time is 200 s.

Characterization

The surface morphology of the as-prepared films were examined by FESEM (JEOL JSM-7100F) at 15 kV. Crystalline phases of the films on substrate were identified by X-ray diffraction (XRD, D8 Advance, Bruker) with Cu $k\alpha$ ($\lambda = 0.15406$ nm) radiation. HRTEM images were obtained on Tecnai F20 FEG-S/TEM. Shimadzu 2200 UV-Vis spectrometer was used to measure the light absorption capabilities of the $\text{Bi}_2\text{Fe}_4\text{O}_9$ electrodes. The steady-state photoluminescence (PL) spectra were measured with a fluorescence spectrophotometer (FLSP-920, Edinburgh Instruments) upon 375 nm light excitation at room temperature. XPS with Al $K\alpha$ ($h\nu = 1253.6$ eV) radiation source was used to characterize the chemical composition of the samples. All the binding energies were calibrated by using C 1s (284.8 eV) as a reference.

(Photo)electrochemical (PEC) measurements

All the (photo)electrochemical measurements were performed on an electrochemical workstation (CHI 660e, CH Instruments, Inc), using a typical three electrode setup with Pt wire as counter electrode and KCl saturated Ag/AgCl electrode as reference electrode. The photocurrent was measured under sunlight simulator (Newport) equipment with AM 1.5G filter at the intensity of 100 mW cm^{-2} . A solution of 1 M NaOH (pH 13.6) was used as electrolyte for all photoelectrochemical and electrochemical measurements. Linear sweep voltammetry (LSV) scans were recorded in a potential window between -0.6 and 0.6 V vs Ag/AgCl at a scan rate of 20 mV s^{-1} . The measured potentials were converted to reversible hydrogen electrode (RHE) using the Nernst equation.²

$$E_{RHE} = E_{Ag/AgCl} + 0.059 * pH + 0.197 V \quad (1)$$

IPCE measurement was obtained using an Oriel Cornerstone 260 1/4 m monochromators with a 300 W Oriel Xenon lamp as the simulated light source. A potential of 1.23 V_{RHE} was applied by a CHI 660e electrochemical workstation and the power density at a specific wavelength was measured by a Newport 1918-c power meter. The IPCE were calculated according to equation 2.³

$$IPCE (\%) = \frac{j (mA cm^{-2}) * 1239.8 (V.nm)}{\lambda (nm) * I (mW cm^{-2})} * 100 \quad (2)$$

j is the photocurrent density (mA cm⁻²) measured from the electrochemical workstation, λ refers to the incident light wavelength (nm), and I is the light density measured at a specific wavelength (mW cm⁻²).

To estimate the effective electrochemically active surface area (ECSA), cyclic voltammograms (CV) scans were measured without illumination in the potential range of 0.74 to 0.94 V vs RHE, where there is no faradaic current at various scan rates (Fig. S4). The ECSA should be proportional to the slope based on equation 3.⁴

$$j = \nu C = (\epsilon S / 4\pi d) \nu \quad (3)$$

j is the charging current, ν is the scan rate, and C is the capacitance which is proportional to the surface area S .

Charge separation and charge injection efficiency calculation

Charge separation efficiency (η_{sep}) represents the fraction of holes that do not recombine with electrons in the bulk and travel to semiconductor electrolyte interface to participate in the oxidation reaction can be calculated according to equation 4.⁵

$$\eta_{sep} = \frac{j_{H_2O_2}}{j_{abs}} \quad (4)$$

Where $j_{H_2O_2}$ is the photocurrent obtained in the presence of H_2O_2 in Fig. S6 and j_{abs} is the rate of photon absorption expressed as the current density, derived from the integration of the light-harvesting efficiency spectra with respect to the AM 1.5 G 100 $mW\ cm^{-2}$ solar spectrum. From the standard AM 1.5 G 100 $mW\ cm^{-2}$ solar spectrum in Fig. S7 and visible light absorption of the BFO photoanodes in Fig. S2, the J_{abs} value is calculated to be 11.0 $mA\ cm^{-2}$ (Table S1).

Based on the photocurrents obtained in 1 M NaOH (j_{NaOH}) in Fig. 3a and in the presence of H_2O_2 ($j_{H_2O_2}$) in Fig. S6, the charge injection efficiency can be calculated using equation 5.⁵

$$\eta_{inj} = \frac{j_{NaOH}}{j_{H_2O_2}} \quad (5)$$

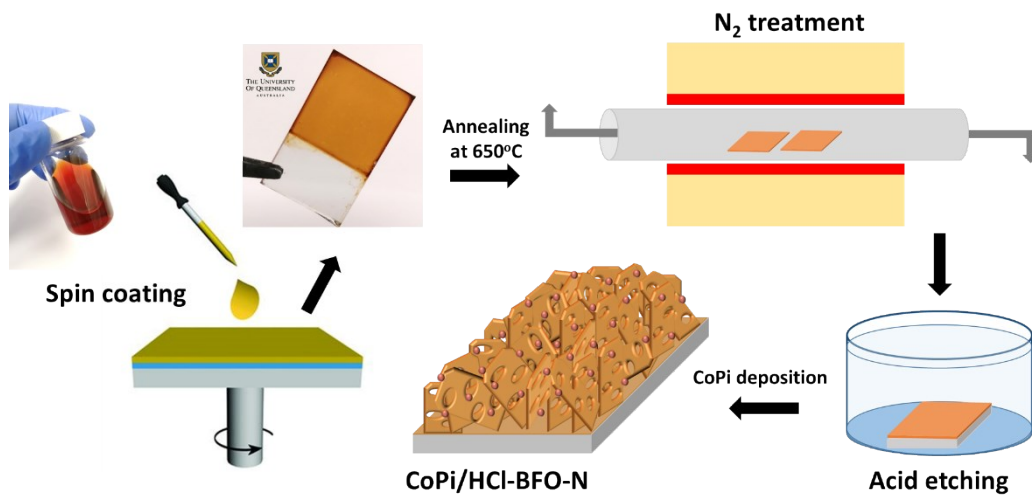


Fig. S1 Fabrication, bulk modification and surface defect engineering of $Bi_2Fe_4O_9$ photoanodes.

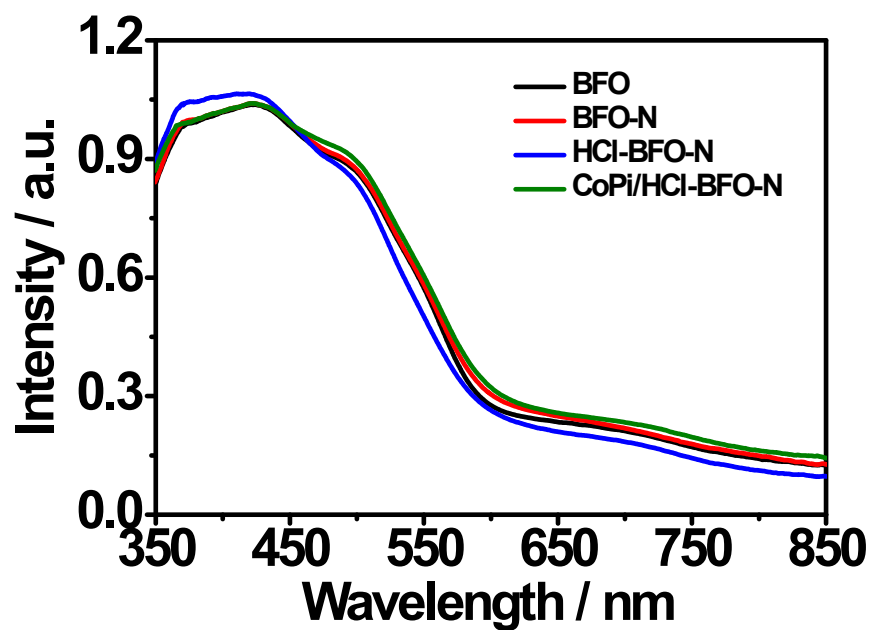


Fig. S2 The light absorption spectra of BFO (black), BFO-N (red), HCl-BFO-N (blue) and CoPi/HCl-BFO-N (green) photoanodes.

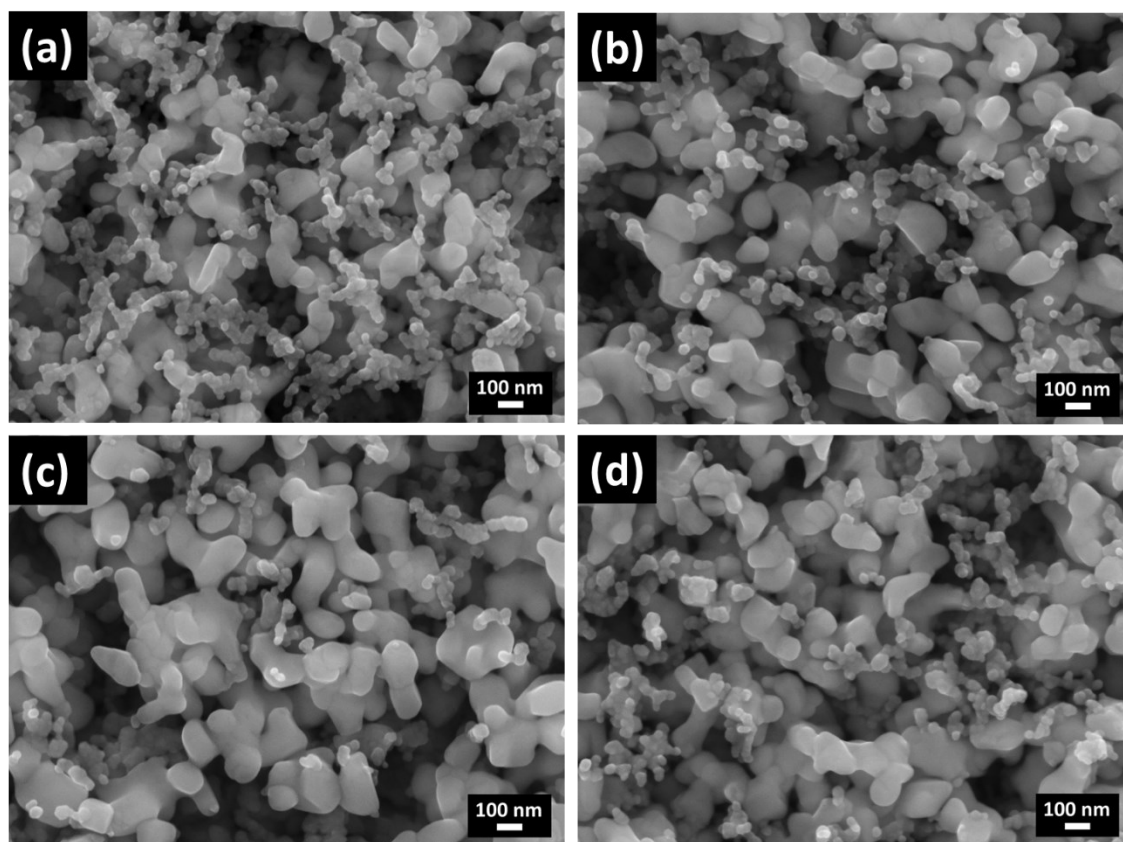


Fig. S3 SEM images of (a) BFO, (b) BFO-N, (c) HCl-BFO-N and (d) CoPi/HCl-BFO-N photoanodes.

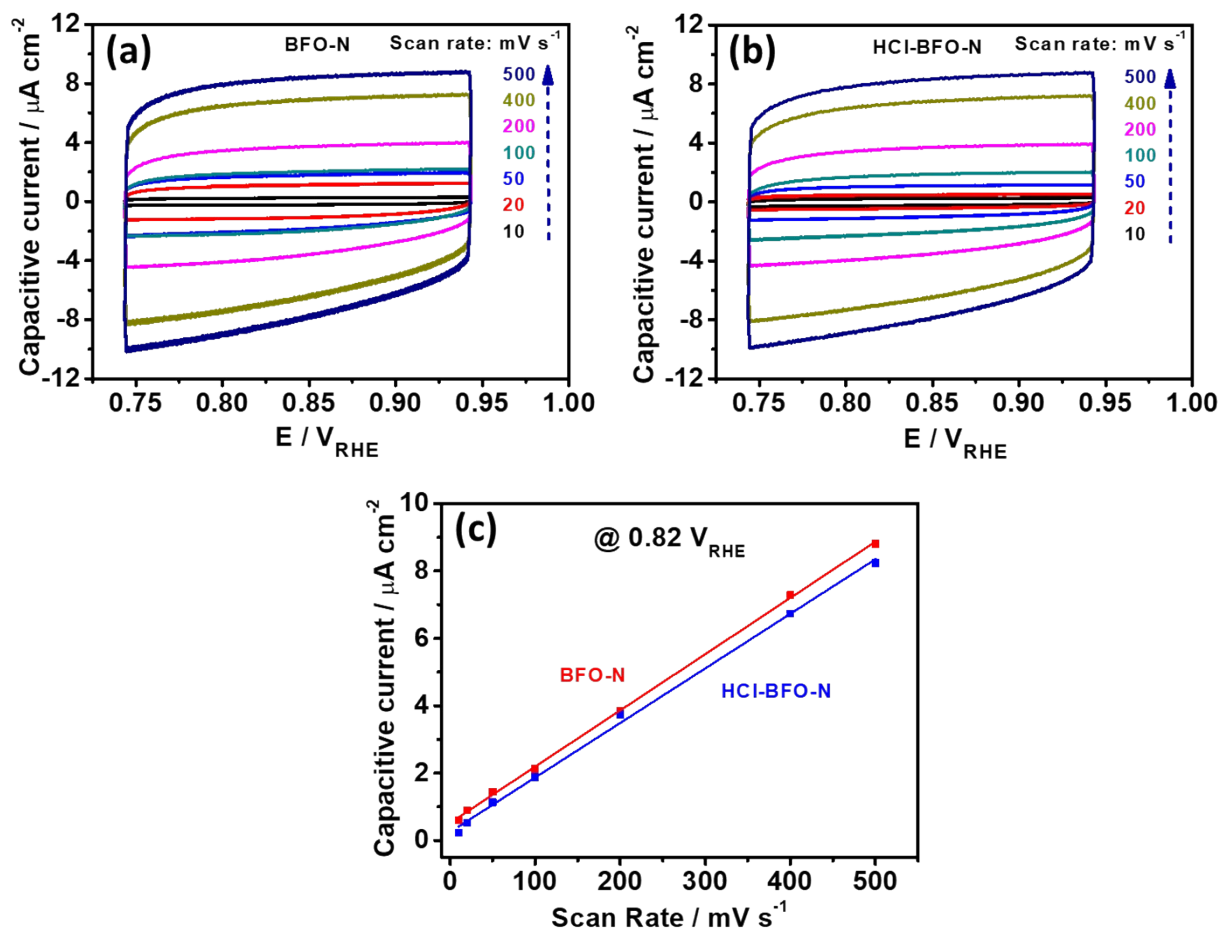


Fig. S4 The CVs of (a) BFO-N, (b) HCl-BFO-N photoanodes at different scan rates ranging from 10 to 500 mV s^{-1} in 1 M NaOH electrolyte and (c) the plots of capacitive current to scan rate for BFO-N (red) and HCl-BFO-N (blue) photoanodes.

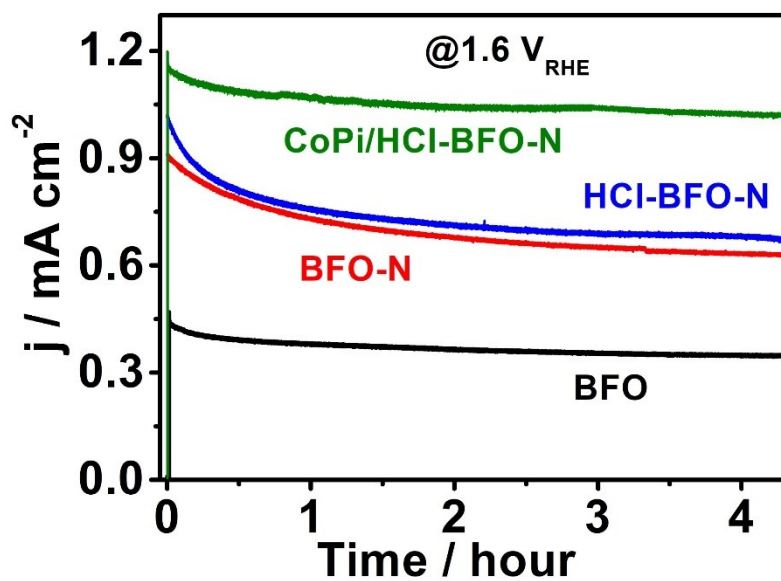


Fig. S5 Stability of BFO (black), BFO-N (red), HCl-BFO-N (blue) and CoPi/HCl-BFO-N (green) photoanodes under AM 1.5 G, 100 mW cm⁻² illumination in 1 M NaOH electrolyte.

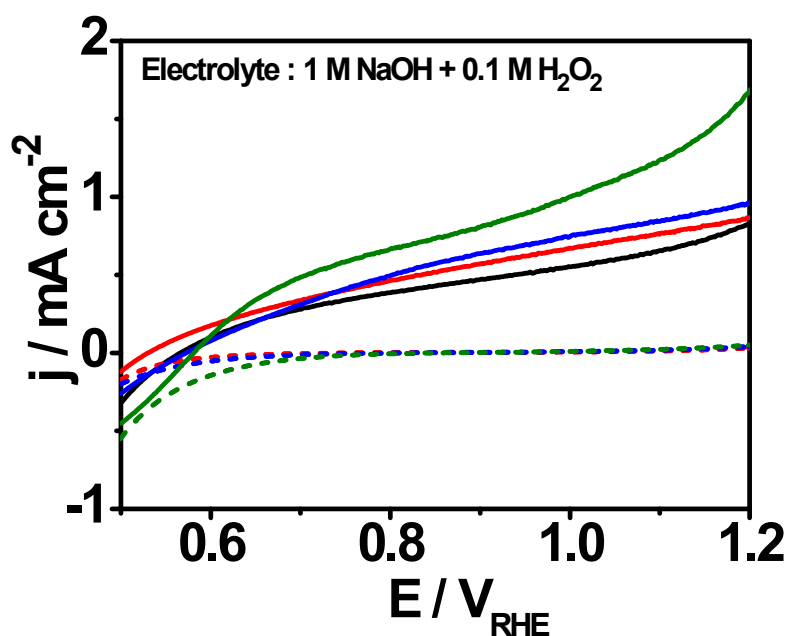


Fig. S6 The photocurrent density of BFO (black), BFO-N (red), HCl-BFO-N (blue) and CoPi/HCl-BFO-N (green) photoanodes in 1 M NaOH the presence of 0.1 M H₂O₂.

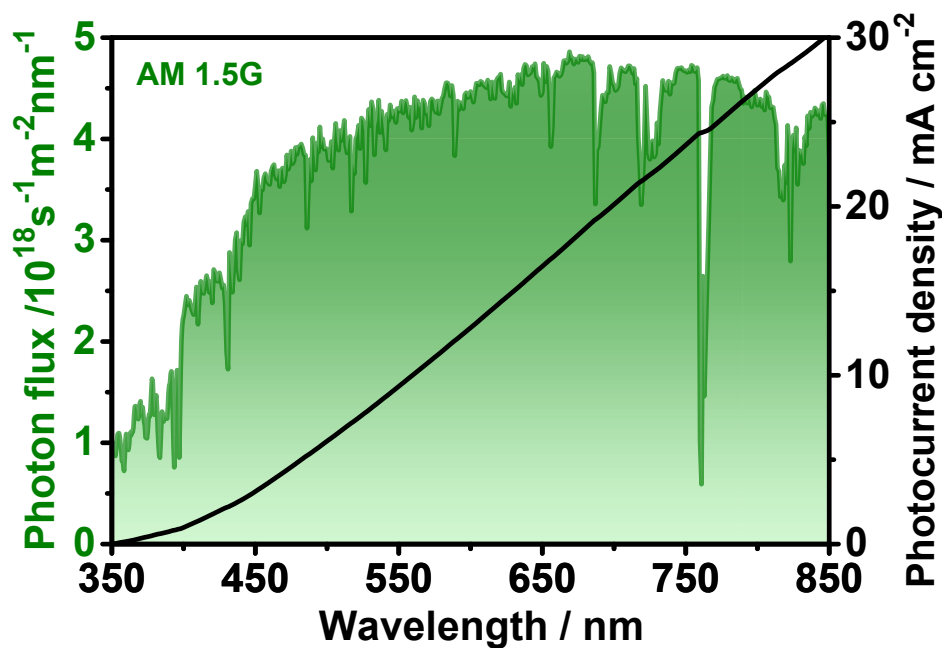


Fig. S7 Integrated photocurrent density of photoelectrodes under the illumination of standard AM 1.5 G, 100 mW cm^{-2} solar spectrum.

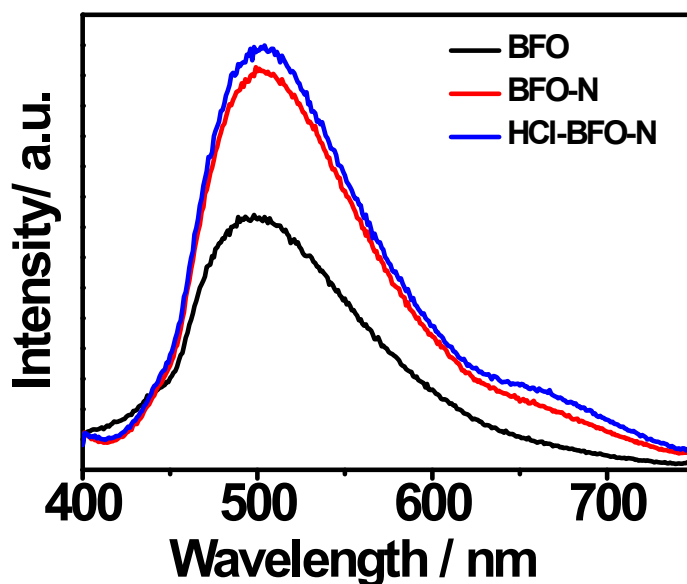


Fig. S8 Photoluminescence emission spectra (excitation wavelength = 375 nm) of BFO (black), BFO-N (red) and HCl-BFO-N (blue) photoanodes.

Table S1: Integrated j_{abs} values for $\text{Bi}_2\text{Fe}_4\text{O}_9$ based photoanodes.

| Photoanodes | $j_{\text{abs}} / \text{mA cm}^{-2}$ |
|----------------|--------------------------------------|
| BFO | 11.0 |
| BFO-N | 11.0 |
| HCl-BFO-N | 10.9 |
| CoPi/HCl-BFO-N | 11.25 |

References

1. Y. Pihosh, I. Turkevych, K. Mawatari, J. Uemura, Y. Kazoe, S. Kosar, K. Makita, T. Sugaya, T. Matsui and D. Fujita, *Sci. Rep.*, 2015, **5**, 11141.
2. X. Lv, L. Tao, M. Cao, X. Xiao, M. Wang and Y. Shen, *Nano Energy*, 2018, **44**, 411-418.
3. Z. Chen, T. F. Jaramillo, T. G. Deutsch, A. Kleiman-Shwarsctein, A. J. Forman, N. Gaillard, R. Garland, K. Takanabe, C. Heske and M. Sunkara, *J. Mater. Res.*, 2010, **25**, 3-16.
4. Z. Wang, Y. Qi, C. Ding, D. Fan, G. Liu, Y. Zhao and C. Li, *Chem. Sci.*, 2016, **7**, 4391-4399.
5. Z. Wang, X. Zong, Y. Gao, J. Han, Z. Xu, Z. Li, C. Ding, S. Wang and C. Li, *ACS Appl. Mater. Interfaces*, 2017, **9**, 30696-30702.